Check for updates

Earthquake Spectra

RESEARCH PAPER

Conversion of Seismic Fragility and Vulnerability Models to Alternative Intensity Measures for Regional Risk Analysis

Gerard J. O'Reilly | Volkan Ozsarac | Davit Shahnazaryan

Centre for Training and Research on Reduction of Seismic Risk (ROSE Centre), Scuola Universitaria Superiore IUSS di Pavia, Pavia, Italy

Correspondence: Gerard J. O'Reilly (gerard.oreilly@iusspavia.it)

Received: 26 November 2025 | **Revised:** 19 April 2026 | **Accepted:** 8 June 2026

Keywords: fragility function | intensity measure conversion | seismic risk | vulnerability modelling

ABSTRACT

Fragility and vulnerability models are key components of regional seismic risk analysis. They relate ground shaking intensity, expressed through an intensity measure (IM) such as spectral acceleration or peak ground velocity, to a probability of damage or loss. When performing a risk analysis for an entire portfolio of structures, these fragility models are often developed based on different IM types for each taxonomy, creating a problematic mismatch in IMs when looking to comparatively evaluate and collectively apply them regionally. Previous research has proposed various approaches for converting fragility functions to a common IM, including methods based on uniform hazard equivalence, total probability, and the use of proxy structures. Another uniform risk equivalence procedure is trialled here along with a more refined consideration of hazard. These methods are systematically compared via 2,260 conversion cases, assessing their ability to convert fragility functions defined with both traditional and next-generation IMs, such as average spectral acceleration, which have yet to be explored. The conversion strategy is also extended and tested for vulnerability model conversion, which is still lacking in the literature. Results show that methods based on uniform hazard and risk equivalence are not consistently reliable, while total probability-based approaches perform better but require detailed hazard information. A key finding is that conversions from suboptimal IMs, such as peak ground acceleration, do not yield improved predictive performance even when mapped to more optimal IMs. Practical guidance and accompanying tools are provided to support analysts in applying and testing these conversion methods for their own fragility and vulnerability models.

1 | Introduction

Seismic risk analysis involves using fragility and loss models to probabilistically describe the potential negative outcomes resulting from earthquake events. These include damage evaluations like structural collapse during seismic shaking, where fragility functions are required, or losses via vulnerability functions. More formally, fragility functions describe the probability of a structure exceeding a given damage state (DS) at a certain intensity of shaking, $P[DS > ds \mid IM = im]$. Likewise, a vulnerability function describes the expected value of loss for a given level of shaking, $E[L \mid IM = im]$. This definition of loss typically refers to economic loss but can be extended to other consequences such as indirect losses, casualties, or business interruption. The conditioning value of intensity in these fragility (or vulnerability) functions is characterised by an intensity measure (IM), which can have various types, including classical definitions like peak ground acceleration (PGA) or spectral acceleration at a given period, Sa(T), or even more generalised definitions like macroseismic intensity. The choice of this IM depends on factors such as structure typology, application purpose, and data availability. The suitability of IMs can be evaluated using several criteria, typically described as sufficiency, efficiency, practicality, and lack of bias. The result of this wide range of IM choices, and the means with which to evaluate their suitability, often yields libraries of fragility (or vulnerability) functions from typology-specific studies, in many cases possessing slightly different IM definitions.

When performing regional risk analysis, where large portfolios of assets are geographically spread across different locations, ground motion fields (GMFs) are simulated based on a stochastic event set. These are combined with catalogues of functions that represent the portfolio, herein referred to as models, to estimate the negative consequences such as loss. Doing this with fragility (or vulnerability) models defined using a plethora of IMs can become challenging. If the assets can be considered independent, their losses are assessed independently using individual IM-specific GMFs and the total loss for the entire portfolio is found by summing all the individual contributions. However, in situations where assets cannot be considered independent, difficulties arise since it means that several cross-correlated GMFs must be simultaneously generated to evaluate the assets collectively. It is not only computationally very demanding to handle a large spatial covariance matrix, but the required models to generate these cross-correlated GMFs are seldom available (e.g., Monteiro and O'Reilly 2026). However, it should be noted that procedures based on conditional hazard that simplify the modelling of GMFs do exist (e.g., [Weatherill et al. 2015]), although these come with the penalty of approximating some correlations (e.g., Goda and Hong 2008). Examples of where such consideration would be needed are for critical infrastructures such as power, gas, water and bridge networks with cascading effects (e.g., Franchin and Cavalieri 2015; Esposito et al. 2015; Abarca et al. 2022, 2025), or when the structure-to-structure damage correlation between buildings is considered (Heresi and Miranda 2022; Mejia and O'Reilly 2026).

Alternatively, it is often simpler and more computationally efficient to define fragility (or vulnerability) models in terms of common IMs so that a single GMF can be used in consequence estimation. This would have the added benefit that fragility/vulnerability models from different sources can be directly compared to visually assess their differences and suitability for specific taxonomies. Standard definitions are typically used, such as PGA or spectral acceleration at a specific period like Sa($T = 0.5$ s). For example, Rosti et al. (2021) used PGA to define fragility models, opting for a practical and pragmatic approach, despite the known issues of sufficiency, efficiency, and bias that have been widely reported in the literature (e.g., Shome et al. 1998; Mehdizadeh et al. 2017; Ghimire et al. 2021; O'Reilly 2021). Also, the Global Earthquake Model global (Martins and Silva, 2021) and the 2020 European seismic risk model (ESRM20) (Crowley et al. 2021) models use several definitions of Sa(T) in their risk models that somewhat mediate these issues that persist with PGA. Nonetheless, these generalised definitions of IM for fragility/vulnerability models still contrast structure-specific IMs like spectral acceleration at the predominant period of vibration Sa($T = \mathrm{T}_1$) or other ad hoc definitions, which often boast increased accuracy through their detailed scrutiny. Furthermore, advancements in vulnerability modelling have indicated that there are several so-called next-generation IMs such as average spectral acceleration, $\mathrm{Sa}_{\mathrm{avg}}(T)$ (e.g., [Eads et al. 2015; Kazantzi and Vamvatsikos 2015]), or filtered incremental velocity, FIV3(T) (Dávalos and Miranda 2019), that have demonstrated much improved accuracy and explanatory power with respect to classic IMs like PGA or Sa(T). Despite these advancements in vulnerability modelling, their use on a regional scale remains limited to date.

Unless systematic vulnerability model development for a wide range of taxonomies is collectively carried out, such as Martins and Silva (2021) and Crowley et al. (2021), risk modellers often face the issue of how to rationally use several different IM definitions in their fragility/vulnerability models when looking to comparatively assess them, or collectively apply them to inter-dependent structural networks. Furthermore, using such generalised and regional approaches to vulnerability modelling, they cannot benefit from the dozens of individual models that are developed for individual research groups based on detailed analysis for specific typologies and IM definitions. Faced with this, the analyst's choices are then to follow three different strategies, assuming the analyst cannot segregate the analysis and perform independent evaluations. The first is to use a single IM for all fragility (or vulnerability) functions, and estimate consequences from a single GMF with these. The second involves using several and more optimised IMs for every fragility/vulnerability function, and estimating consequences from several cross-correlated GMFs with these. This is despite these cross-correlated models being seldom available and difficult to generate (Monteiro and O'Reilly 2026), although Monteiro et al. (2026) have recently proposed a spatial correlation model that greatly reduces this challenge in practical implementation. Lastly, the third approach is to adopt fragility (or vulnerability) functions from several ad hoc sources, each potentially using a different IM, and convert them to a single generalised IM. This would significantly increase the computational efficiency of regional analysis since it would require only a single GMF type to be simulated. Furthermore, the generalised IM could potentially take forms other than the classic PGA which has persisted for several decades.

This paper discusses this last issue in detail, examining past research on model conversion and exploring the topic further to form practical advice for risk modellers. Some methods for conversion of fragility functions have been previously proposed, but have focused on the conversions between traditional IM definitions (e.g., Sa(T) and PGA) via different simplified schemes. One of the most notable contributions was provided by Suzuki and Iervolino (2020), who employed a total probability approach. However, to date no study has thoroughly investigated conversions beyond these spectral-based IMs and next-generation IMs that have emerged as promising alternatives in recent years. The present study builds upon these foundational insights, but differs in scope and objectives. While Suzuki and Iervolino (2020) primarily focused on the formulation of fragility conversion using scalar and vector-valued IMs, as well as on the accuracy of such conversions under controlled settings, this work adopts a risk-modelling perspective aimed at providing practical guidance for risk modellers. In doing so, it explores a range of conversion settings and methods based on a single IM, reflecting the fact that the vast majority of fragility functions available in practice are developed using a single IM. In addition, other more simple approaches based on assumptions of uniform hazard and uniform risk equivalence are trialled to investigate whether any practical usage can be made of these for IM conversion strategies in practical application. In particular, this paper (i) systematically compares multiple conversion strategies in terms of both accuracy and practical effort with 2,260 individual cases, (ii) examines the influence of hazard disaggregation detail and IM efficiency on conversion reliability, (iii) extends the analysis to next-generation IMs, and (iv) explores the direct conversion of vulnerability models in addition to underlying fragility functions. Through applications to 2,260 individual cases that give a more holistic view of the problem being tackled, the paper provides practical guidance for risk modellers on when and how IM conversion can be reliably applied, and where its limitations should be acknowledged.

2 | Review of Existing Conversion Methods

2.1 | Uniform Hazard Equivalence

The need to compare and cross-evaluate different fragility contributions has been known for several years. This was highlighted in the SYNER-G project (Pitilakis et al. 2014) in Europe when Silva et al. (2014) proposed a fragility function manager tool to collect and compare fragility functions developed using different methodologies from various sources in the literature. While the objective was to create a centralised database and resource for risk modellers, it also addressed the issue regarding the lack of IM uniformity across the available fragility functions. Silva et al. (2014) proposed a scaling factor based on the 2006 international building code (IBC) design spectrum (IBC 2006) that is applied to the fragility function's median value, and illustrated in Figure 1, although no detailed studies were conducted to verify the accuracy of such approach. Similar strategies were proposed for peak ground velocity (PGV) and spectral displacement. O'Reilly and Calvi (2020) also proposed a similar methodology that was instead based on a comparison of the IM hazard curves resulting from probabilistic seismic hazard analysis (PSHA), also shown in Figure 1. The main advantage of this over the Silva et al. (2014) approach is that a more refined definition of the IM hazard is employed and non-Sa(T)-based IMs can also be considered. Although it involves slightly more complex input data, the same underlying approximation remains, and no rigorous testing was carried out by the authors to verify the accuracy of such approach, at least with respect to simpler version proposed in Silva et al. (2014).

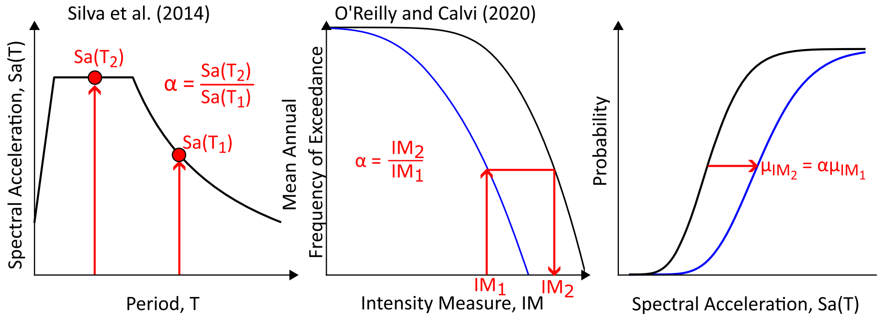

FIGURE 1 | Illustration of the uniform hazard conversion methodologies described in Silva et al. (2014) and O'Reilly and Calvi (2020).

These approximate approaches are based on equivalent uniform hazard and the assumption of equal variability among the two fragility functions (i.e., the original and the converted fragility function). This means that if an analyst has a fragility function defined in terms of Sa(1 s) via a lognormal distribution with median η and dispersion β, and wishes to convert it to Sa(0.5 s), they would simple keep the same dispersion β and linearly scale the median value by the factor α (Figure 1). The median intensity is therefore scaled based on its relative uniform hazard spectrum-based value. It neglects aspects of differences in variability for the IMs themselves, along with potentially different rupture contributions, and assumes all IMs are equally efficient, which is known not to be the case.

2.2 | Uniform Risk Approach

Building on the uniform hazard approach, a risk-consistent approach is trialled in this study. It is based on the fact that risk, or more formally the mean annual frequency of exceedance, λ, of a DS is unique for a given structure and site location regardless of the conditioning IM employed. This was initially shown by both Bradley (2012) and Lin et al. (2013) and requires that the IM employed is efficient, sufficient, and unbiased, and that the ground motion records used in the analysis are hazard-consistent.

If the fragility function is represented via a lognormal distribution with median and dispersion, η and β, and the hazard curve is represented as a log-linear relationship $H = k_0 \mathrm{im}^{-k_1}$, Cornell et al. (2002) solved for λ as shown below

$$\lambda_{\mathrm{DS}} = \int_0^{+\infty} \mathrm{P}[\mathrm{DS} \mid \mathrm{IM} = \mathrm{im}] \mid \mathrm{dH}(\mathrm{IM}) \mid \tag{1}$$

$$= k_0 \eta^{-k_1} \exp\left(0.5 k_1^2 \beta^2\right) \tag{2}$$

and since $\lambda_{\mathrm{DS}}^{\mathrm{IM}_1}$ can be taken as equal to $\lambda_{\mathrm{DS}}^{\mathrm{IM}_2}$ for two different IMs, this equivalence is extended here to give

$$\lambda_{\mathrm{DS}}^{\mathrm{IM}_1} = \lambda_{\mathrm{DS}}^{\mathrm{IM}_2} \tag{3}$$

$$k_{0,\mathrm{IM}_1} \eta_{\mathrm{IM}_1}^{-k_{1,\mathrm{IM}_1}} \exp\left(0.5 k_{1,\mathrm{IM}_1}^2 \beta_{\mathrm{IM}_1}^2\right) = k_{0,\mathrm{IM}_2} \eta_{\mathrm{IM}_2}^{-k_{1,\mathrm{IM}_2}} \exp\left(0.5 k_{1,\mathrm{IM}_2}^2 \beta_{\mathrm{IM}_2}^2\right) \tag{4}$$

$$\eta_{\mathrm{IM}_2} = \left(\frac{k_{0,\mathrm{IM}_1} \eta_{\mathrm{IM}_1}^{-k_{1,\mathrm{IM}_1}} \exp\left(0.5 k_{1,\mathrm{IM}_1}^2 \beta_{\mathrm{IM}_1}^2\right)}{k_{0,\mathrm{IM}_2} \exp\left(0.5 k_{1,\mathrm{IM}_2}^2 \beta_{\mathrm{IM}_2}^2\right)} \right)^{\frac{-1}{k_{1,IM_2}}} \tag{5}$$

Typically, the parameters of one fragility function, η_{IM1} and β_{IM1}, are known, meaning that a single equation is solved for two parameters, η_{IM2} and β_{IM2}. A simple approach may be to assume a fixed value of dispersion β_{IM2} and solve for η_{IM2}, which will be trialled here. In addition, the second-order development of Cornell et al. (2002)'s solution in Equation (1) proposed by Vamvatsikos (2013) can also be utilised for improved accuracy, and will be utilised here.

2.3 | Proxy Structure Analysis

Karaferis and Vamvatsikos (2022) presented a novel method to convert fragility functions via proxy structure analysis. This requires developing an equivalent single-degree of freedom (SDOF) structure and the assumption of fundamental properties like period, strength, and DS definition. Analysts must perform many trials and iterate towards identifying an equivalent SDOF structure that would result in the same fragility function as the candidate fragility to be converted. Once identified, this equivalent SDOF structure's analysis results can be recomputed in terms of the target fragility function IM. This is essentially doing a conversion of a proxy structure that is intended to represent the actual original fragility function and does not actually work on the original fragility function directly. It also requires little to no hazard information to implement, beyond selecting suitable ground motions for the SDOF analysis making it an attractive alternative. Karaferis and Vamvatsikos (2022) conducted several case studies and noted a good overall performance of the methodology.

2.4 | Total Probability Approach

The previous methods each rely on simplifying assumptions regarding hazard, risk, and uncertainty to devise an equivalence between IMs. To address this, proposals were made based on an application of the total probability theorem as follows

$$P[\mathrm{DS} \mid \mathrm{IM}_2] = \int_{\mathrm{IM}_1} P[\mathrm{DS} \mid \mathrm{IM}_1] f_{\mathrm{IM}_1 \mid \mathrm{IM}_2} \, d\mathrm{IM}_1 \tag{6}$$

where $P[\mathrm{DS} \mid \mathrm{IM}_1]$ is the original fragility function based on IM_1, and $f_{\mathrm{IM}_1 \mid \mathrm{IM}_2}$ is the conditional distribution of IM_1 given IM_2 to result in the converted fragility function $P[\mathrm{DS} \mid \mathrm{IM}_2]$. This was initially presented in Michel et al. (2018), albeit with an error[1], which was later noted and corrected by Suzuki and Iervolino (2020), who then further expanded and tested this formulation with 24 conversion cases of $\mathrm{Sa}(T)$, which Michel et al. (2018) did not conduct.

It is well-known from ground motion selection studies that the conditional distribution $f_{\mathrm{IM}_1 \mid \mathrm{IM}_2}$ depends on the underlying rupture parameters. Therefore, Suzuki and Iervolino (2020) further extended Equation (6) to include the magnitude, M, and rupture distance, R, as follows

$$P[\mathrm{DS} \mid \mathrm{IM}_2] = \int_{\mathrm{IM}_1} \int_{\mathrm{M}} \int_{\mathrm{R}} P[\mathrm{DS} \mid \mathrm{IM}_1, \mathrm{M}, \mathrm{R}] f_{\mathrm{IM}_1, \mathrm{M}, \mathrm{R} \mid \mathrm{IM}_2} \, d\mathrm{IM}_1 \, d\mathrm{M} \, d\mathrm{R} \tag{7}$$

where the conditional distribution term $f_{\mathrm{IM}_1, \mathrm{M}, \mathrm{R} \mid \mathrm{IM}_2}$ was rearranged to a more familiar format of

$$f_{\mathrm{IM}_1, \mathrm{M}, \mathrm{R} \mid \mathrm{IM}_2} = f_{\mathrm{IM}_1 \mid \mathrm{IM}_2, \mathrm{M}, \mathrm{R}} \, f_{\mathrm{M,R} \mid \mathrm{IM}_2} \tag{8}$$

where $f_{\mathrm{IM}_1 \mid \mathrm{IM}_2, \mathrm{M}, \mathrm{R}}$ is the conditional distribution of IM_1 given IM_2 and the rupture parameters M and R. This conditional distribution is already widely used in the conditional spectrum (CS) or generalised conditional intensity measure (GCIM) ground motion selection approaches (Lin et al. 2013; Bradley 2010). The $P[\mathrm{DS} \mid \mathrm{IM}_1, \mathrm{M}, \mathrm{R}]$ term implies that the fragility function is also a function of rupture parameters M and R. For most IMs, these are assumed to be sufficient (Luco and Cornell 2007) and hence independent of rupture parameters, meaning it can be simply written as $P[\mathrm{DS} \mid \mathrm{IM}_1]$ herein. The $f_{\mathrm{M,R} \mid \mathrm{IM}_2}$ term is computed via the disaggregation of the PSHA results for IM_2 in terms of M and R. Suzuki and Iervolino (2020) noted that this strictly refers to the *occurrence* of $\mathrm{IM}_2 = \mathrm{im}_2$ and not its exceedance $\mathrm{IM}_2 > \mathrm{im}_2$ as is typically done. Interested readers are referred to Fox et al. (2016) for further information on the implications of either approach. While magnitude and distance are pertinent parameters from the hazard disaggregation that impact the conditional distribution $f_{\mathrm{IM}_1, \mathrm{M}, \mathrm{R} \mid \mathrm{IM}_2}$, a further step to generalise and include all scenario parameters (e.g., soil condition, rake, and hypo-central depth), and ground motion models (GMMs) is proposed here and they are collectively termed *Rup* through the generalised form

$$\begin{aligned} P[\mathrm{DS} \mid \mathrm{IM}_2] &= \int_{\mathrm{IM}_1} \int_{\mathrm{Rup}} P[\mathrm{DS} \mid \mathrm{IM}_1] f_{\mathrm{IM}_1, \mathrm{Rup} \mid \mathrm{IM}_2} \, d\mathrm{IM}_1 \, d\mathrm{Rup} \\ &= \int_{\mathrm{IM}_1} \int_{\mathrm{Rup}} P[\mathrm{DS} \mid \mathrm{IM}_1] f_{\mathrm{IM}_1 \mid \mathrm{IM}_2, \mathrm{Rup}} f_{\mathrm{Rup} \mid \mathrm{IM}_2} \, d\mathrm{IM}_1 \, d\mathrm{Rup} \end{aligned} \tag{9}$$

This extends Suzuki and Iervolino (2020) to capitalise on the complete disaggregation output format of the OpenQuake engine (Pagani et al. 2014), where instead of using basic information on the relative contributions of only M and R to the hazard, all rupture scenario parameters and associated GMMs are used. With some simple programming tools available in the associated GitHub repository, this can be exploited for a more thorough implementation of Equation (9). Suzuki and Iervolino (2020) also considered the case where a vector-based fragility function defined in terms of both IM_1 and IM_2, $P[\mathrm{DS} \mid \mathrm{IM}_1 \cap \mathrm{IM}_2]$, is available, and showed that it can be rewritten using only IM_2 by exploiting this same conditional distribution of IM_1 given IM_2; essentially, the vector-based fragility function is reduced to a scalar IM expressed solely in terms of IM_2.

The $f_{\mathrm{Rup} \mid \mathrm{IM}_2}$ term in Equation (9) is computed by disaggregating the PSHA results in terms of IM_2 occurrence, whereas $f_{\mathrm{IM}_1 \mid \mathrm{IM}_2, \mathrm{Rup}}$ is computed as in the CS and GCIM ground motion selection approaches as the conditional distribution with a mean and variance (assuming a lognormal distribution) as follows

$$f_{\mathrm{IM}_1 \mid \mathrm{IM}_2, \mathrm{Rup}} \sim \mathcal{N}\left(\mu_{\ln \mathrm{IM}_1 \mid \ln \mathrm{IM}_2, \mathrm{Rup}}, \sigma^2_{\ln \mathrm{IM}_1 \mid \ln \mathrm{IM}_2, \mathrm{Rup}}\right) \tag{10}$$

$$\mu_{\ln \mathrm{IM}_1 \mid \ln \mathrm{IM}_2, \mathrm{Rup}} = \mu_{\ln \mathrm{IM}_1 \mid \mathrm{Rup}} + \rho_{\ln \mathrm{IM}_1, \ln \mathrm{IM}_2} \sigma_{\ln \mathrm{IM}_1 \mid \mathrm{Rup}} \epsilon_{\ln \mathrm{IM}_2 \mid \mathrm{Rup}} \tag{11}$$

$$\epsilon_{\ln \mathrm{IM}_2 \mid \mathrm{Rup}} = \frac{\ln im_2 - \mu_{\ln \mathrm{IM}_2 \mid \mathrm{Rup}}}{\sigma_{\ln \mathrm{IM}_2 \mid \mathrm{Rup}}} \tag{12}$$

$$\sigma^2_{\ln \mathrm{IM}_1 \mid \ln \mathrm{IM}_2, \mathrm{Rup}} = \sigma^2_{\ln \mathrm{IM}_1 \mid \mathrm{Rup}} \left(1 - \rho^2_{\ln \mathrm{IM}_1, \ln \mathrm{IM}_2}\right) \tag{13}$$

where $\mu_{\ln \mathrm{IM}_1 \mid \mathrm{Rup}}$ and $\sigma_{\ln \mathrm{IM}_1 \mid \mathrm{Rup}}$ are the mean and standard deviation of IM_1 using a single GMM and rupture parameter set, $\rho_{\ln \mathrm{IM}_1, \ln \mathrm{IM}_2}$ is the correlation coefficient between the two IMs and is typically assumed as independent of Rup parameters (e.g., [Baker and Bradley 2017; Aristeidou et al. 2025]). The epsilon term, $\epsilon_{\ln \mathrm{IM}_2 \mid \mathrm{M,R}}$, represents the number of standard deviations above or below the mean GMM prediction of $\mathrm{IM}_2 = \mathrm{im}_2$.

In short, an original fragility function defined in terms of IM_1 can be transformed to a converted fragility in terms of IM_2 by applying Equation (9). Here, for a given value of $\mathrm{IM}_2 = \mathrm{im}_2$, and for each value of IM_1 considered as part of the integral, Equations (11)–(13) are applied for each Rup case to compute the conditional distribution $f_{\mathrm{IM}_1 \mid \mathrm{IM}_2, \mathrm{Rup}}$ via Equation (10). Integrating this with the original fragility function $\mathrm{P}[\mathrm{DS} \mid \mathrm{IM}_1]$ returns the complete distribution $\mathrm{P}[\mathrm{DS} \mid \mathrm{IM}_2]$.

3 | Extension to Vulnerability Modelling

The previous section described an application of the total probability theorem to convert a fragility function defined in terms of IM_1 to a different IM_2. Research on the topic to date has focused on the conversion of fragility functions, where a specific DS and its associated distribution are described. However, in many instances, fragility functions alone do not fully describe the seismic risk of a structure, and vulnerability functions describing economic loss or other consequences are usually adopted. Furthermore, the conversion methodology described in Section 2.4 typically assumes that the original fragility function $\mathrm{P}[\mathrm{DS} \mid \mathrm{IM}_1]$ is described via lognormal distribution with median and dispersion values η_{IM1} and β_{IM1}. In the case of vulnerability functions, this is usually not the case, and a discrete distribution of expected values of loss versus intensity of shaking $\mathrm{E}[\mathrm{L} \mid \mathrm{IM}]$ are typically described. Since many risk models work directly in terms of vulnerability and not fragility, it is also of interest to extend the fragility-based conversion approach to a vulnerability-based conversion and test its robustness, which to the authors' knowledge has not been examined in past research. This is done here, where the expression given in Equation (9) is extended to give

$$\mathrm{E}[\mathrm{L} \mid \mathrm{IM}_2] = \int_{\mathrm{IM}_1} \int_{\mathrm{Rup}} \mathrm{E}[\mathrm{L} \mid \mathrm{IM}_1]\, f_{\mathrm{IM}_1 \mid \mathrm{IM}_2, \mathrm{Rup}}\, f_{\mathrm{Rup} \mid \mathrm{IM}_2}\, \mathrm{dIM}_1\, \mathrm{dRup} \tag{14}$$

where the $\mathrm{E}[\mathrm{L} \mid \mathrm{IM}_1]$ represents the *original* vulnerability function and $\mathrm{E}[\mathrm{L} \mid \mathrm{IM}_2]$ is the *converted*, with all other terms being the same as before.

4 | Methodology

Following the methodologies presented, the following set of methods were trialled below to convert the fragility/vulnerability functions from an original IM_1 to a new IM_2:

- **Method 1** is the total probability approach described in Section 2.4. It uses the full disaggregation information obtained from OpenQuake (i.e., not limited to M and R utilised by Suzuki and Iervolino (2020)) defined in terms of occurrence and the correlation model of Aristeidou et al. (2025), hence is termed the "exact" approach using Equation (9), given its probabilistic basis and scrutiny with respect to hazard information.
- **Method 2** follows the same approach as Method 1, but with three much simpler considerations of the hazard disaggregation information to investigate whether any notable penalty in conversion accuracy is incurred with respect to using the exact approach:
  - **Method 2a** uses enough rupture scenarios so that 50% of the hazard is accounted for;
  - **Method 2b** uses the mean M, R, and GMM scenario from the disaggregation;
  - **Method 2c** uses the modal M, R, and GMM scenario from the disaggregation.
- **Method 3** tests the Silva et al. (2014) proposal described in Section 2.1, where the dispersion is maintained constant and the median value's conversion is done based on relative IBC spectrum values. This will only be done to convert $\mathrm{Sa}(T)$-based IMs;
- **Method 4** tests the O'Reilly and Calvi (2020) approach presented in Section 2.1, where the dispersion is maintained constant and the median's scaling is based on the hazard curves computed via PSHA for each candidate IM;
- **Method 5** approaches the problem with the equal risk approximation postulated in Section 2.2, where the dispersion is assumed to be equal to the original IM_1 and the median value is calculated to harmonise the risk computed using two fragility functions.

Of all the methods presented above, it should be stressed that Method 1 is expected to be the most accurate one since it is based on the total probability theorem and considers all rupture scenario parameters available from hazard analysis. The other methods represent potential simplifications and alternative approximations that may be useful in some cases, and whose overall usefulness in practical application will be commented on later. The Karaferis and Vamvatsikos (2022) methodology, while promising and potentially useful in structure-specific studies, was not trialled given its ambiguity in defining suitable DS thresholds and other input criteria.

5 | Analysis

5.1 | Overview of Case Study

Using each of these conversion methodologies, a series of case study structures (Section 5.2) were analysed. Nonlinear response history analysis (Section 5.3) was applied and fragility functions were developed (Section 5.4) for each structure. These are defined in terms of several original IMs, defined as: peak absolute quantities, PGA, and PGV; spectral acceleration at several periods, Sa(0.5 s), Sa(1 s), Sa(1.5 s), Sa(2 s); filtered incremental velocity at several periods, FIV3(0.5 s), FIV3(1s), FIV3(1.5 s), FIV3(2 s); two alternative definitions of average spectral acceleration as described in Shahnazaryan and O'Reilly (2024) at several periods, $Sa_{avg2}(0.5\,s)$, $Sa_{avg2}(1\,s)$, $Sa_{avg2}(1.5\,s)$, $Sa_{avg2}(2\,s)$, and $Sa_{avg3}(0.5\,s)$, $Sa_{avg3}(1\,s)$, $Sa_{avg3}(1.5\,s)$, $Sa_{avg3}(2\,s)$.

Each of these original fragility functions defined in terms of IM_1 was transformed to the converted fragility function in terms of IM_2 and compared to its corresponding IM_1 reference equivalent. For example, a structure was analysed to develop a fragility model in terms of both $IM_1 = Sa(0.5\,s)$ and $IM_1 = PGA$. The $IM_1 = Sa(0.5\,s)$ set was converted to $IM_2 = PGA$ and evaluated against the $IM_1 = PGA$ reference case. This comparison was made for many cases (i.e., four models, eighteen IMs, five DSs, and seven conversion methodologies to give a total of 2,260 conversion cases) where the comparison is generally made graphically. This comparison was also quantified in terms of the fitted lognormal parameters for both IM_1 and IM_2, which are the median η (or lognormal mean μ) and lognormal standard deviation β. Illustrative comparisons are shown to facilitate discussion, with graphical results for all cases available on the GitHub repository. For a more concise summary here, the Hellinger distance (Hellinger 1909) was employed to summarise all results and give a better sense of the overall patterns. It describes the similarity between the fragility functions for IM_1 and IM_2, denoted $F_{IM1} \sim \mathcal{N}(\mu_1,\beta_1^2)$ and $F_{IM2} \sim \mathcal{N}(\mu_2,\beta_2^2)$, and is defined as

$$H\left(F_{IM_1},F_{IM_2}\right) = \sqrt{1-\sqrt{\frac{2\beta_1\beta_2}{\beta_1^2+\beta_2^2}}\exp\left(-\frac{1}{4}\frac{(\mu_1-\mu_2)^2}{\beta_1^2+\beta_2^2}\right)} \tag{15}$$

The Hellinger distance ranges from 0 (identical distributions) to 1 (completely disjoint distributions), making it a useful metric for gauging how the overall similarity between *original* and *converted* fragility functions can be interpreted for all cases analysed.

In all cases, the fragility functions will be converted from IM_1 to IM_2 using the methodologies described above, in addition to the vulnerability function being converted using the methods described in Section 3.

5.2 | Structural Systems

Several SDOF systems with varying characteristics were considered. Each system was modelled in OpenSees and Figure 2a presents the backbone curves along with the model identifiers and fundamental periods. Models (1)–(3) used a uniaxial bilinear *Hysteretic* material with pinching factors of 0.8 and 0.5 for strain and stress, respectively, during reloading. Model (3) also accounted for damage based on energy dissipation. Model (4) utilised a uniaxial *Pinching4* material, incorporating damage accumulation as a function of energy dissipation. A damping ratio of 5% was applied using tangent stiffness proportional damping.

For each structural system, five DSs were considered. DS1 was assumed to initiate at 75% of the yielding displacement. Significant damage (DS4) corresponds to the onset of fracturing, while intermediate DSs were evenly spaced between DS1 and DS4. Complete damage (DS5) was assumed to occur at the system's ultimate displacement capacity. For each of these DSs, it was assumed that the structure has been damaged to a fraction of its overall replacement value via a *damage-to-loss model*, or *consequence model*. These are denoted $E[L \mid DS_i]$ for DS_i and when combined with the fragility functions, the

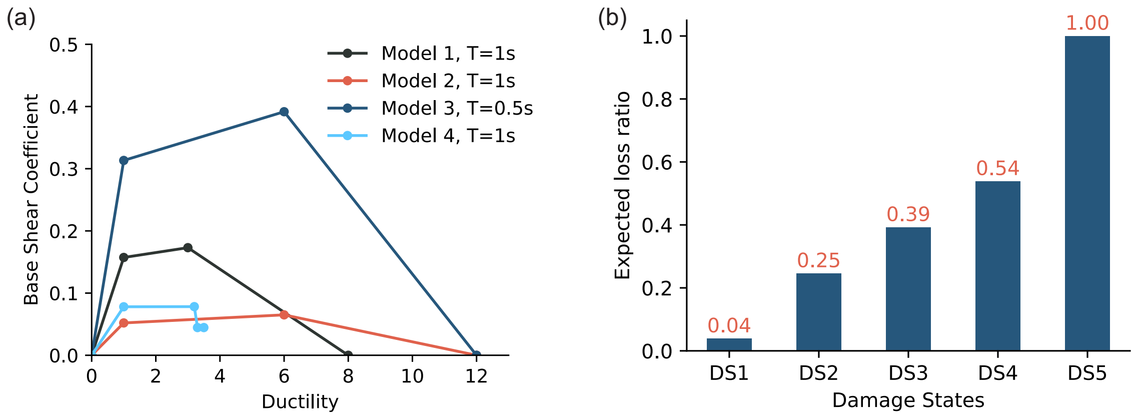

FIGURE 2 | (a) Backbone curves of the SDOFs utilised for nonlinear dynamic analyses and (b) damage-to-loss model.

expected loss ratio versus intensity is obtained to give the vulnerability function via Equation (16). This study adopted the damage-to-loss model from O'Reilly and Shahnazaryan (2024), shown in Figure 2b.

$$E[L_T \mid IM] = \sum_i E[L \mid DS_i] P[DS_i \mid IM] \tag{16}$$

5.3 | Characterisation of Seismic Hazard

To characterise the seismic hazard and select ground motion records for the analysis required to develop the fragility/vulnerability models, PSHA was performed using the OpenQuake engine (Pagani et al. 2014) for the site of L'Aquila, Italy. In particular, the seismic source model ZS9 proposed by Meletti et al. (2008) for the seismic hazard assessment of Italy (Stucchi et al. 2009, 2011) was adopted. The adopted ground motion logic tree collapses to a single branch, defined using the GMM by Aristeidou et al. (2024), developed for active shallow crustal regions. This choice was motivated by the model's ability to predict the next-generation IMs of interest in the present work. The hazard curves for each IM previously described are shown in Figures 3 and 4 illustrate a sample disaggregation in terms of both exceedance and occurrence for Sa(1.0s) at 10% probability of exceedance (POE) in 50 years.

A set of 40 ground motion records (single component) was selected from the NGA West-2 database (Ancheta et al. 2014) for each IM and POE level. These followed the CS method using the Djura Record Selector (https://apps.djura.it) (Shahnazaryan et al. 2025). Figure 3 also shows the hazard consistency checks for the ground motion record set selected for IM = Sa(1.0 s), where a good agreement was observed across all IMs considered in this study. Similar plots for all other IMs are available in the GitHub repository.

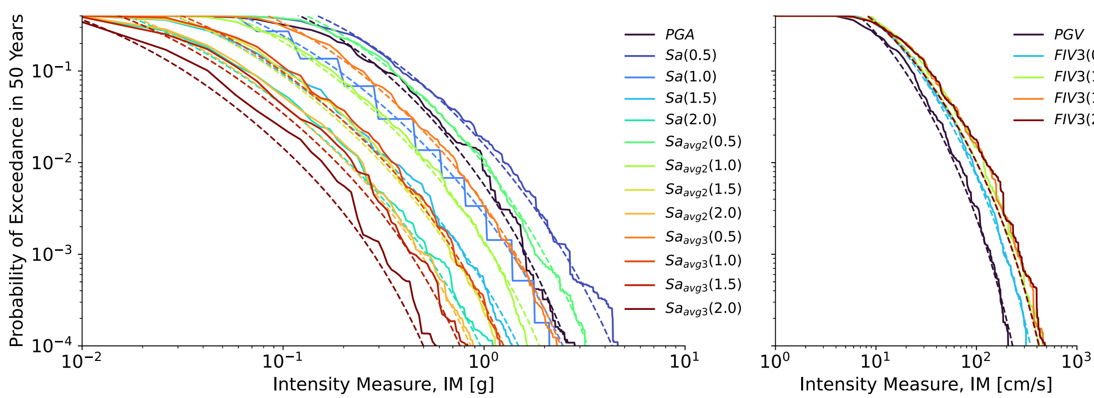

FIGURE 3 | Hazard curves for each IM considered (dashed lines) alongside the hazard consistency checks (solid lines) for the selected ground motion record set conditioned on IM = Sa(1.0s).

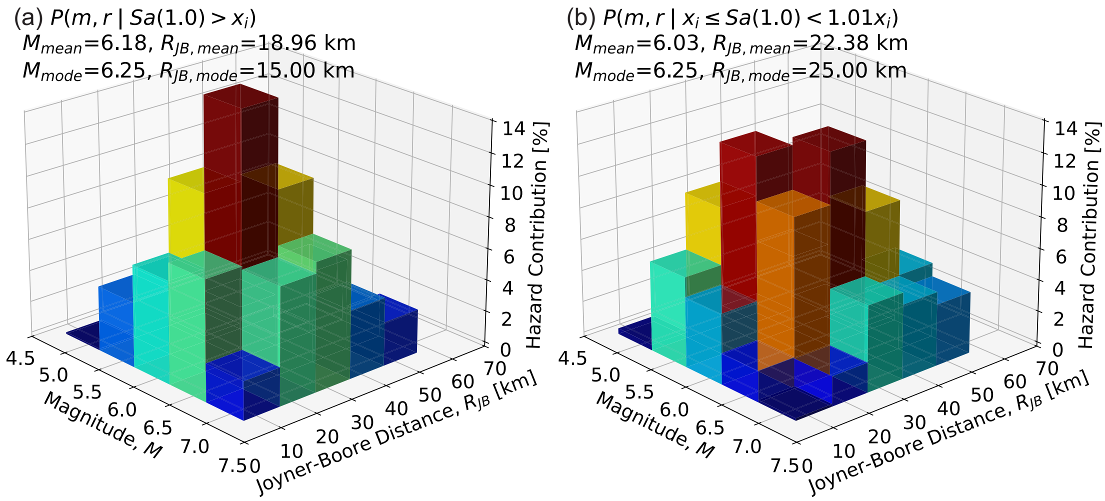

FIGURE 4 | Seismic hazard disaggregation for Sa(1.0s): (a) Sa(1.0s) > x_i and (b) $x_i \leq$ Sa(1.0s) < 1.01 · x_i where x_i = 0.19g.

5.4 | Numerical Analysis and Fragility/Vulnerability Modelling

Multiple stripe analysis (MSA) was carried out using the ground motion record sets identified in Section 5.3 on the structural systems described in Section 5.2. For each structural model, fragility functions were developed for each DS considered and ground motion record set. With these MSA results for each combination and the DS definitions previously described, fragility functions were developed by counting the number of exceedances of system's DS threshold at each IM level, and fitting a lognormal distribution to the data via maximum likelihood estimation. Likewise, using the damage-to-loss model shown in Figure 2b, the vulnerability functions were also derived using Equation (16).

6 | Model Conversion Results

6.1 | Fragility Function Comparisons

To first examine the comparisons of each method listed in Section 4, Figure 5 shows a single conversion case, where the fragility functions for a single structure's DS are converted from $IM_1 = Sa(1.0)$ to $IM_2 = PGA$ and then compared to the reference fragility function initially developed in terms of $IM_1 = PGA$. Also shown for each conversion case are the Hellinger distances, as per Equation (15).

In general, there is some variability between the approaches examined, with the most refined approach (Method 1) visually matching closely, as confirmed by the low Hellinger distance. This observation confirms that implementing the total probability approach is indeed effective for converting the IM of fragility functions. Methods 2a, 2b, and 2c, which are similar to Method 1 but with much reduced consideration of seismic hazard information, also show good agreement. This

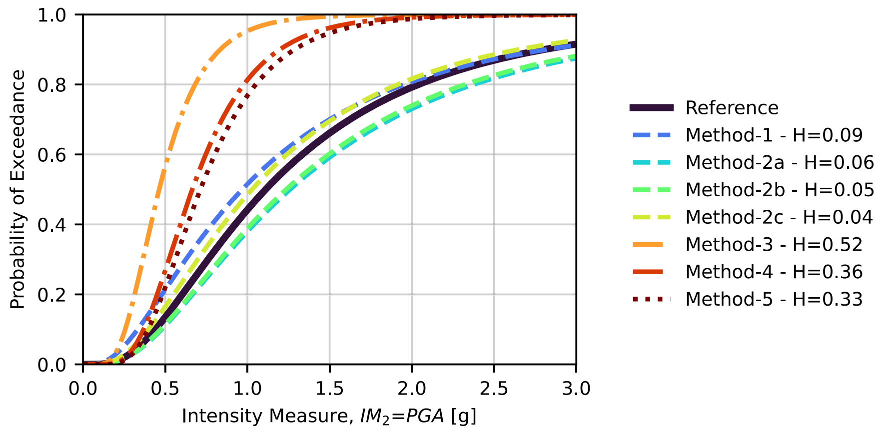

FIGURE 5 | Comparison of reference (IM_1 = PGA) and converted (from IM_1 = Sa(1.0) to IM_2 = PGA) fragility functions for Model 2 at DS5.

confirms the results previously presented in Suzuki and Iervolino (2020), who performed a similar conversion between these IM types, albeit for different structures and seismic hazard. There are some differences but the overall match is quite good. For Methods 3, 4, and 5, on the other hand, their limitations are evident, as the matching is relatively poor for this specific case. This stems from the assumption that the dispersion was equal to the initial $IM_1 = Sa(1.0\ s)$ value, despite the fact that a more inefficient $IM_2 = PGA$ was being sought; hence, a higher dispersion would have been expected. Methods 1 and 2 captured this shift in dispersion, whereas the other methods did not. Additionally, the median value is quite different, meaning that a simple scaling based on uniform hazard is also not always guaranteed to work and is case specific, as will be shown next. A brief note of caution is made regarding the Hellinger distances shown in Figure 5 since it shows that Methods 2a–2c are apparently more accurate than Method 2 due to the lower value, despite Method 2 being a simpler implementation of Method 1. This difference, while relatively low, was due to the fitting error between the discrete data obtained from each of the conversion methods and the subsequent fitting of a lognormal distribution that was evaluated.

To present a more general view of the methodologies, Figure 6 presents a similar conversion using a single model and DS but for different $IM_1 - IM_2$ pairs. The vertical axis of the plot grid indicates the original IM_1 and the horizontal axis indicates the converted IM_2, meaning that the first row, second column (starting from the bottom left) shows the case of an $IM_1 = Sa(2.0\ s)$ fragility function converted to $IM_2 = Sa(0.5\ s)$. Overall, the results confirm the observations made in

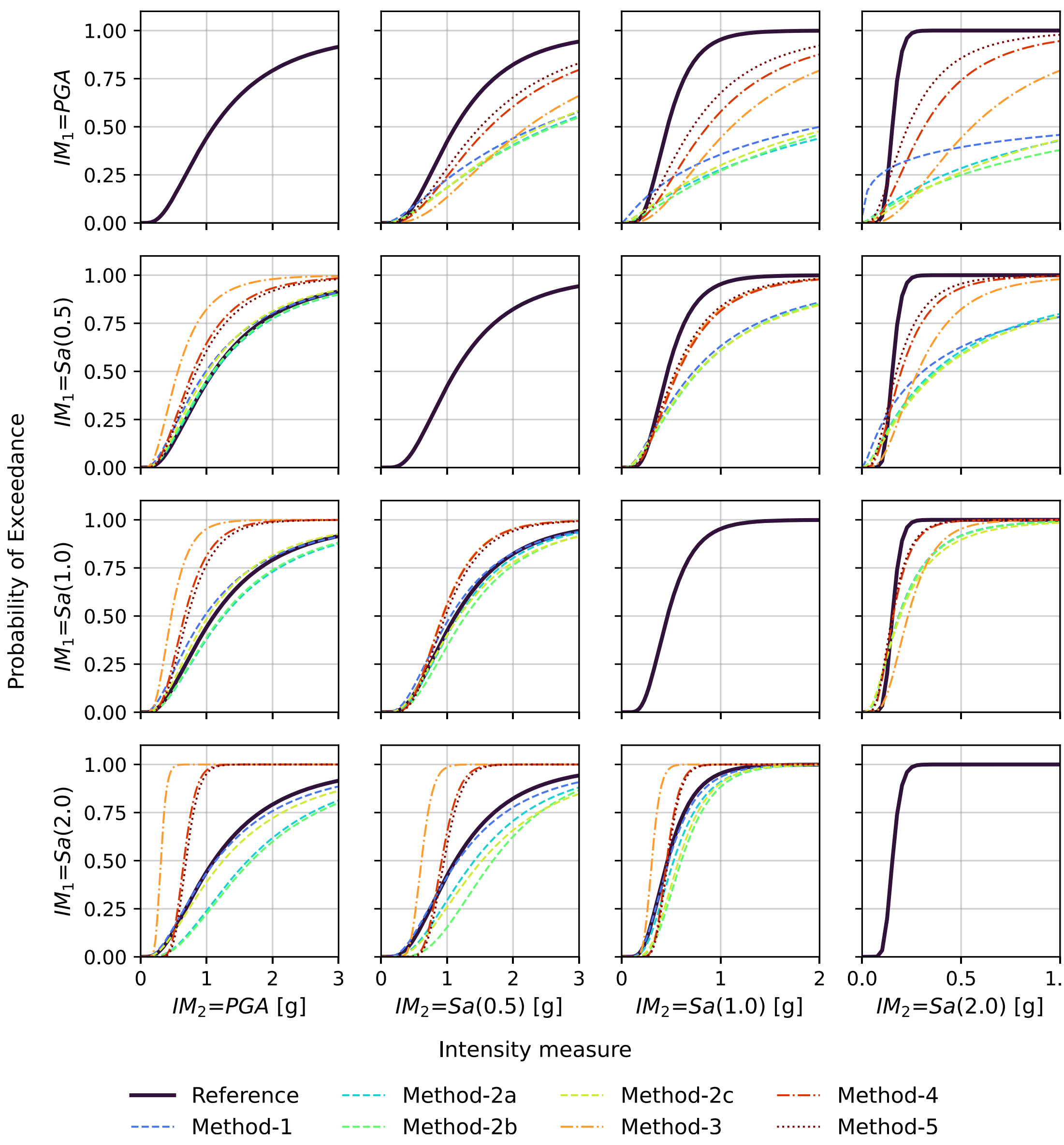

FIGURE 6 | Comparison of reference and converted fragility functions for Model 2 at DS5 using traditional IMs such as PGA and Sa(T).

Figure 5. Methods 3, 4, and 5 tended to match in some cases, particularly when the level of dispersion was similar between the IM_1 and IM_2 pairs, but worsened as these deviated. This is particularly true for cases where all methods have comparable conversions, making the choice of conversion approach less critical given that next-generation IMs have high efficiency and sufficiency. Methods 1 and 2, on the other hand, showed promising results once again; in particular, the results shown in the lower triangle of the plot grid in Figure 6 illustrated very good matching. This corresponds to cases where an $Sa(T)$-based IM is converted to a shorter period of vibration (e.g., $IM_1 = Sa(1\,s)$ to $IM_2 = Sa(0.5\,s)$). There is no clear advantage of considering all possible hazard scenarios as required by Method 1, with each variation of Method 2 also illustrating comparable accuracy, indicating that such scrutiny with respect to seismic hazard disaggregation input information may be relaxed when adopting a total probability approach. For the upper triangle of Figure 6, which corresponds to cases where an $Sa(T)$-based IM is converted to a higher period of vibration (e.g., $IM_1 = Sa(0.5\,s)$ to $IM_2 = Sa(2.0\,s)$), the accuracy of each conversion methodology tends to break down. This trend was observed for all structures examined at each DS considered, where the complete set of plots is available on the GitHub repository. These results also confirm the observations of Suzuki and Iervolino (2020), who made $Sa(T)$-based conversions from $Sa(T_1)$ to $Sa(T_2)$, and noted that when $T_1 > T_2$ (i.e., the lower triangle case of Figure 6), the results tended to be generally good. When $T_1 < T_2$ (i.e., the upper triangle case of Figure 6), the conversions tended to be quite poor. This was attributed to the fact that, in such cases, the conditional distribution becomes wide and poorly constrained, forcing the conversion integral to operate in extrapolation regions where the scalar IM cannot represent the true structural response. In these cases, Methods 3–5 may at first appear to give more reasonable conversions, but further scrutiny reveals this is an artefact of the constant dispersion assumption, which constrains how poorly these methods can perform and is not a reflection of superior conversion methodology. The result in this case is a false impression of better performance, which in the broader scheme of cases analysed is still rather poor. Suzuki and Iervolino (2020) alleviated this issue by constructing vector-valued fragility surfaces using a hybrid linear-logistic model before performing the conversion, highlighting the need for additional scrutiny when converting to IMs at longer vibration periods.

In addition to the $Sa(T)$-based conversion of fragility functions presented in Figure 6 and past literature, this study also investigated next-generation IMs such as $FIV3(T)$ and $Sa_{avg}(T)$, alongside PGV. Figure 7 illustrates some of these conversion cases for a single structure and DS, but the overall trends were observed to be similar for the other cases not presented.

First, examining the methods (excluding Method 3, since it converts only $Sa(T)$-based IMs), it is clear that each conversion strategy achieves a similar level of accuracy across almost all cases. That is, whereas Methods 4 and 5 tended to perform poorly compared to Methods 1 and 2 when applied to traditional IMs (Figure 6), Figure 7 shows that when converting between next-generation IMs, there was no significant difference or loss in accuracy. This was found to be due to the much higher efficiency (i.e., lower dispersion) of these next-generation IMs in characterising the structural damage. Since the overall variability was low across the IM_1–IM_2 pairs, simply converting median values under either uniform hazard or risk equivalency was not a bad approximation. Looking at the individual comparisons, PGV is seen to be an IM that is relatively easy to convert to, regardless of the method employed. $Sa_{avg2}(1.0\,s)$ also appeared to be relatively consistent in its conversion results, both to and from. The only case that illustrated subpar performance was when converting from $IM_1 = Sa_{avg2}(0.5\,s)$ to $IM_2 = FIV3(1.0\,s)$, where the more refined Methods 1 and 2 did not perform so well, especially when compared to Methods 4 and 5, although this is attributed to the same issue of converting from short period IMs to longer period ones.

6.2 | Overall Results

While the previous section presented cases of fragility function conversion for specific IM pairs within a given structural model and DS, this section presents overall comparisons in a more holistic manner using the Hellinger distance described in Equation (15). These are plotted in Figure 8 as the average value across each DS and method presented, and for all IM combinations considered. In short, red indicates a case where the conversion matched poorly to the reference fragility, and green indicates a good conversion. Method 5 is not presented for plotting convenience (although its results are available on the associated GitHub repository), and also since the results closely resembled those of Method 4, which was previously observed in Figures 6 and 7.

Overall, when using fragility functions based on $IM_1 = PGA$, regardless of the method employed, their conversion to any other IM_2 does not work well. This is because of the efficiency and sufficiency issues typically present when using PGA, and this loss of information when characterising fragility functions in terms of PGA cannot be recovered when converting to a more effective IM. Because of this, it is strongly recommended not to develop fragility models for regional application in terms of PGA, as their flexibility is very limited. On the other hand, for most other IM_1 types, converting to $IM_2 = PGA$

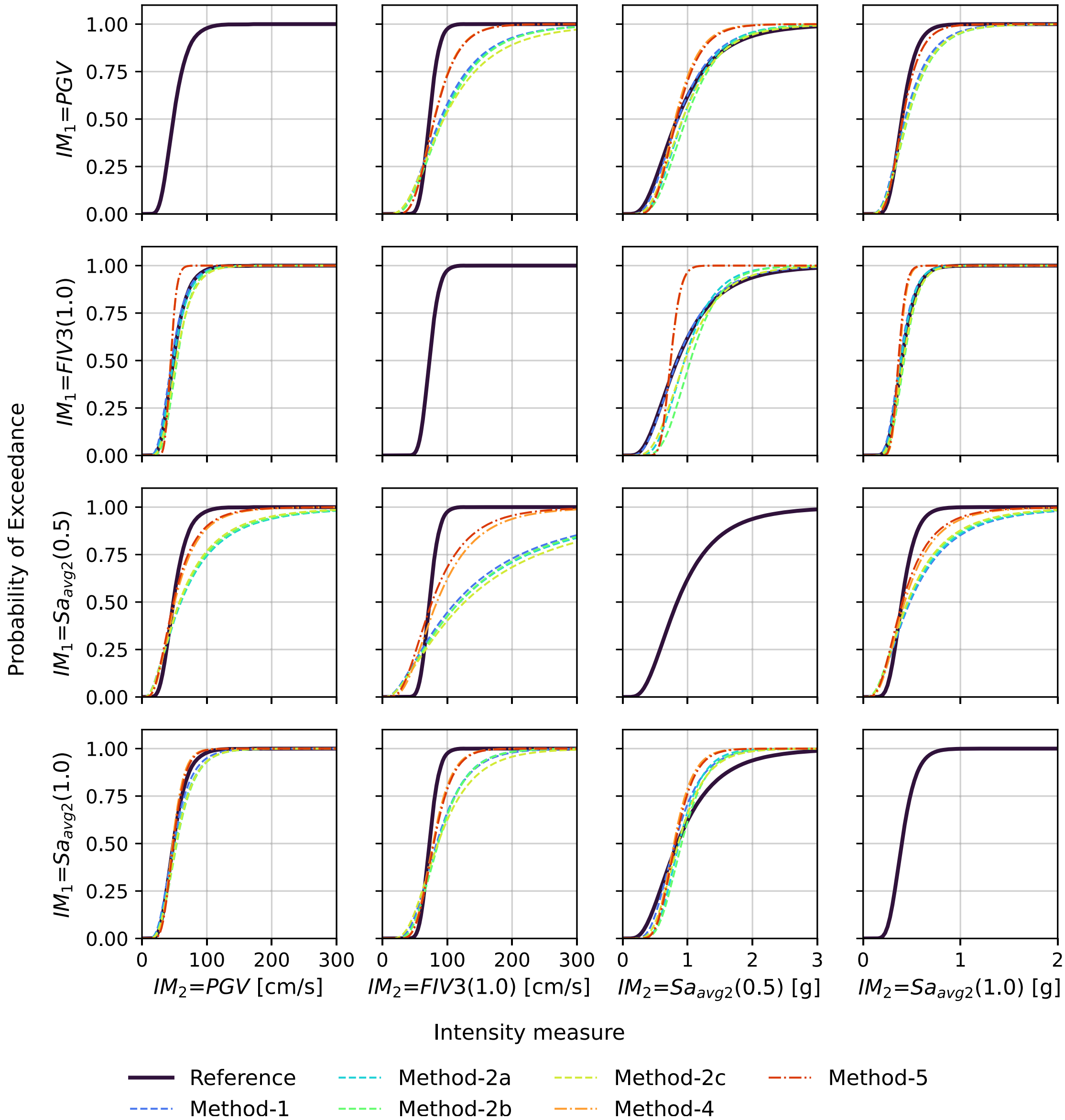

FIGURE 7 | Comparison of reference and converted fragility functions for Model 2 at DS5 using next-generation IMs such as FIV3, and $\mathrm{Sa_{avg}}(T)$.

seems to be very feasible, with the exception of Methods 3, 4, and 5. This means that if fragility models are characterised using more efficient IMs like Sa(0.5) and Sa(1.5s), converting them to a common denominator in PGA is not a bad solution. This is due to the increased explanatory power of these other IMs that render it suitable to relate to the less accurate PGA. The overall variability of the converted fragility functions will still be high, but the conversion methodology should still work well.

This same observation can also be made for $\mathrm{IM_1} = \mathrm{Sa}(0.5\,\mathrm{s})$, where attempting to convert to anything other than PGA is problematic. On the other hand, converting from higher period values of $\mathrm{Sa}(T)$ to a lower period tended to work well across the board, where the reverse case was not true, confirming the early comments made in reference to Figure 6. These same comments about intra-IM period conversions also apply to $\mathrm{Sa_{avg}}(T)$, where converting to lower period values worked well, but to longer periods not. It is worth noting that this applies to cases where $\mathrm{IM_1} = \mathrm{IM_2} = \mathrm{Sa_{avg}}(T)$, since cases where $\mathrm{IM_1} = \mathrm{Sa_{avg}}(T)$ and $\mathrm{IM_2} = \mathrm{Sa}(T)$ showed good conversion results, suggesting that the increased efficiency of $\mathrm{Sa_{avg}}(T)$ made it a flexible candidate to develop fragility functions initially.

Conversions between all versions of $\mathrm{FIV3}(T)$ are very good, which was somewhat expected given that Aristeidou et al. (2025) has shown it to be an IM that is highly correlated with itself for different period values. This means it can almost be considered period-independent, and the results in Figure 8 show that switching between definitions of $\mathrm{FIV3}(T)$ was easily

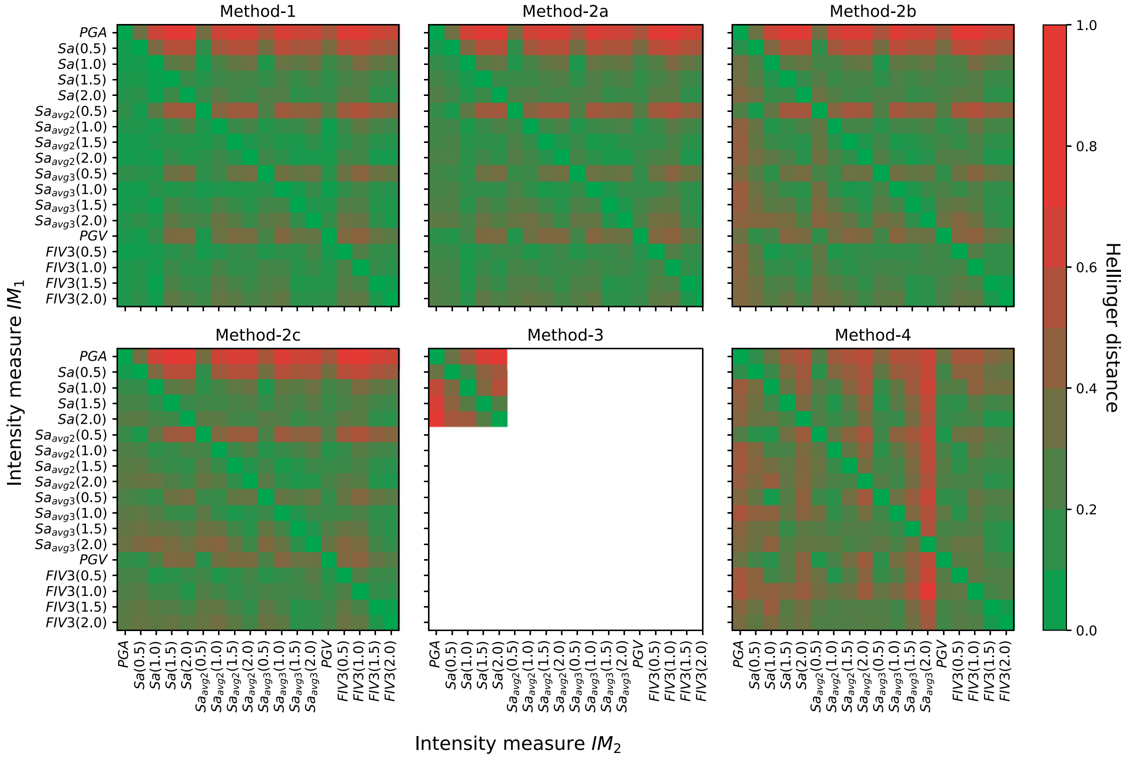

FIGURE 8 | Average Hellinger distances between the reference and the converted fragility functions (from IM_1 to IM_2), computed as the mean of distances across DSs, for Model 2.

done using all methods shown. When scrutinising the conversion between FIV3(T) and other IMs, a curious observation can be made. It can be seen that when $\mathrm{IM}_1 = \mathrm{FIV3}(T)$, converting to any other IM_2 type works very well, regardless of the conversion method adopted, which is completely opposite to the PGA case. To adopt terminology used in blood transfusions, PGA can be thought of as a universal receiver, where FIV3(T) can be thought of as a universal donor. As before, where it was recommended to avoid developing fragility models in terms of PGA, since it offers almost no conversion flexibility and poor efficiency and sufficiency, it is instead recommended to develop fragility models in terms of FIV3(T) since it offers excellent conversion flexibility and has been shown to be an efficient, sufficient, and explanatory IM in many different contexts (e.g., Dávalos and Miranda 2020, 2021; Aristeidou and O'Reilly 2024; Montemayor et al. 2025, 2026). Its relative period independence means that a single value, such as $T = 1$ s, could be used for all structural typologies, without much loss in accuracy.

6.3 | Vulnerability Functions

While the previous sections examined the conversion of fragility functions from one IM to another, with the different methodologies reviewed in Section 2 exhibiting varying levels of conversion accuracy depending on the case considered, this section extends this consideration to vulnerability functions. This is because, while fragility functions are a key component of seismic risk models, vulnerability models are often presented as the final output when assessing risk and consequences, such as monetary losses. Section 3 described this extension via Equation (14), where it was illustrated how an original vulnerability function defined as $\mathrm{E}[\mathrm{L} \mid \mathrm{IM}_1]$ can be converted to $\mathrm{E}[\mathrm{L} \mid \mathrm{IM}_2]$ with analogous considerations of hazard and conditional dependence. This was applied using the previously described Methods 1 and 2, and the original vulnerability functions were derived from the original fragility functions using Equation (16).

Figure 9 illustrates these comparisons in a way that is analogous to Figure 7. What is immediately apparent is that there is no significant difference between the methods employed, indicating that a simpler consideration of seismic hazard may suffice. Overall, the conversion works quite well when moving between different IMs. This is much more pronounced in the case of fragility functions, and an encouraging point is that the matching of lower, more frequent intensities seems reasonable in each case. To further understand this, the average annual loss (AAL) was computed for each case by integrating the vulnerability function with the seismic hazard quantified in Section 5.3. Figure 10 shows the difference of the converted vulnerability functions AAL with respect to the reference vulnerability function that is being matched.

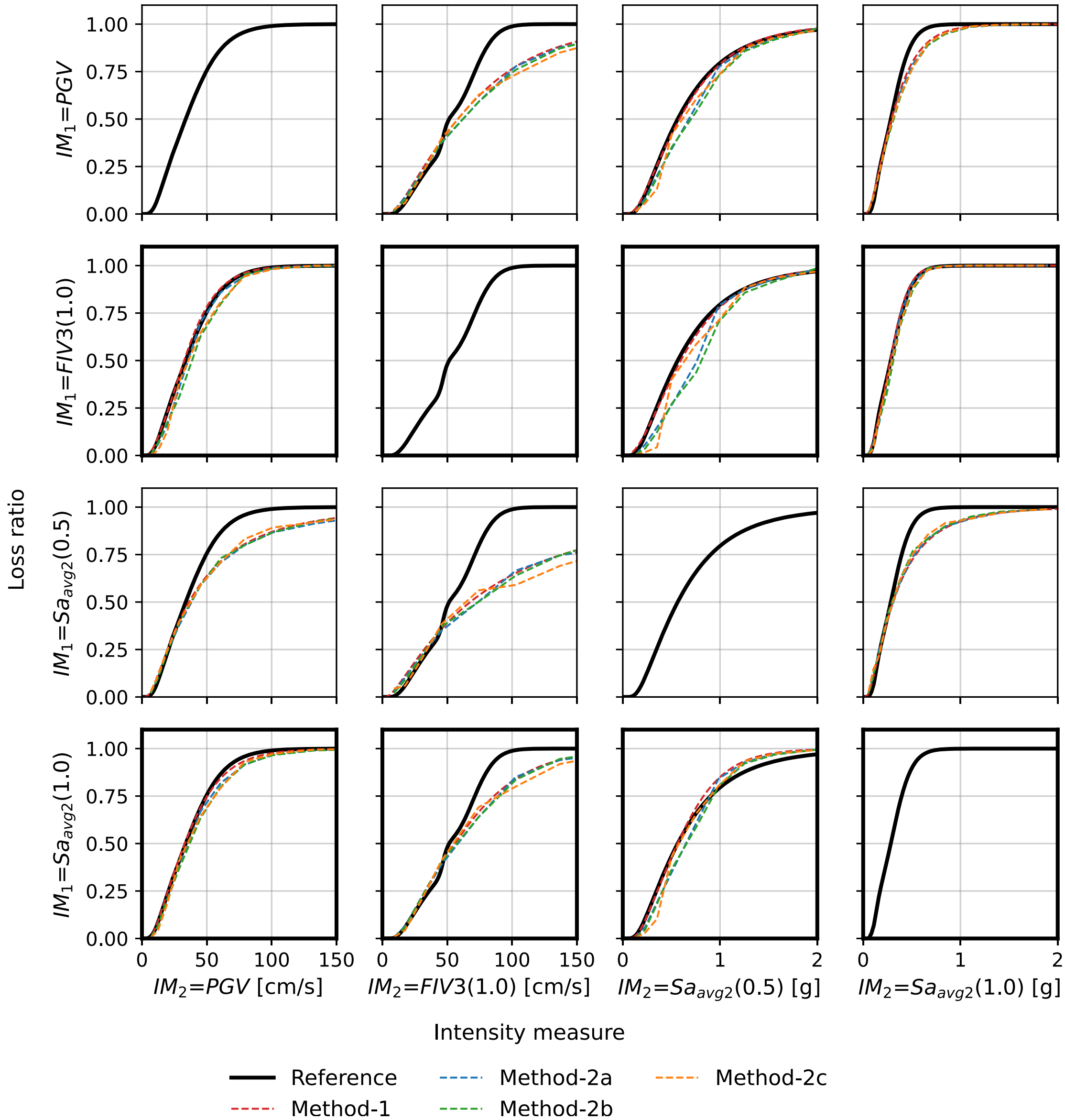

FIGURE 9 | Comparison of reference and converted vulnerability functions for Model 2 using next-generation IMs such as FIV3 and $Sa_{avg}(T)$.

Overall, many of the same observations hold, but a notable point again concerns PGA. Figure 8 previously showed that converting from PGA to any other IM did not work well, but that converting different IMs to PGA was not a bad solution as they matched the reference model. Figure 10, on the other hand, shows that doing this results in a significant overestimation of the AAL. This is caused by the increased uncertainty in PGA, which increases the expected losses for a given IM level, and when integrated with the hazard, inflates the AAL. Therefore, the solution of harmonising fragility models in terms of PGA may seem attractive, but when extended to losses and AAL, it is shown to grossly overestimate. On the contrary, the previous observation of FIV3(T) being a universal donor IM still holds, and maintains good accuracy for the cases examined. Utilising $Sa_{avg}(T)$ as the original IM also showed good conversions, further stating the case for these next-generation IMs to be integrated in vulnerability modelling. All in all, it appears that the vulnerability function conversion is less prone to systematic errors for most IMs compared to fragility functions, meaning that risk modellers can and may wish to focus their conversion here, rather than fragility, which has been studied to date in the literature.

7 | Remarks

Overall, there is no single solution to the issues initially outlined. When multiple fragility or vulnerability models are defined using different IMs, analysts must choose an approach to enable comparison and collective application; in such

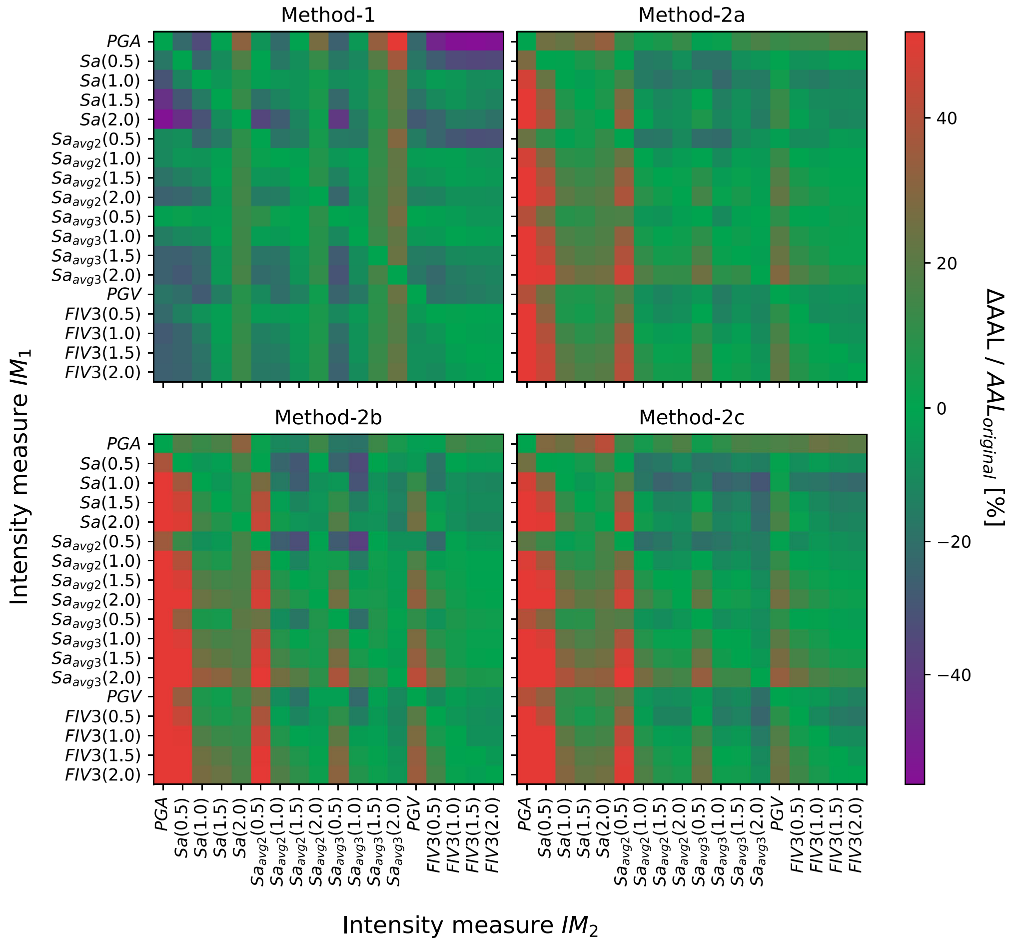

FIGURE 10 | AAL ratio for vulnerability function conversions IM_1 to IM_2 for Model 2.

cases, methods based on total probability should be preferred. Historically, the option of adopting a single IM has been common, with *PGA* being the most widely used over recent decades. However, efficiency and sufficiency considerations have highlighted significant limitations in using PGA to characterise seismic vulnerability. The results presented here further demonstrate how restrictive model definition becomes when using this IM, since it complicates fragility function conversion and can substantially overestimate losses when converted models are applied. An alternative is to use next-generation IMs such as $Sa_{avg}(T)$ or FIV3(T), which retain the practicality of adopting a unique IM while avoiding many of the biases and constraints associated with PGA. This reinforces the case for future fragility and vulnerability modelling to incorporate these improved IMs.

The conversion methods investigated employed different strategies, ranging from assumptions of uniform hazard to uniform risk and also the application of total probability. The total probability approach performed best, although it requires more detailed seismic hazard information, which is often available but not always, confirming earlier observations by Suzuki and Iervolino (2020). Methods 2a, 2b, and 2c, however, indicated that a comprehensive description of hazard disaggregation information is not always needed. Simpler methods can work at times (i.e., Methods 3, 4, and 5), but their success depends heavily on the relative efficiency of the original and target IMs, which governs the reliability of the conversion. Methods 3 and 4 were expected to perform modestly, which was confirmed. Greater expectations were placed on the feasibility of Method 5, as it is grounded in the principle of uniform risk equivalence; however, this ultimately did not materialise into a usable method. Table 1 gives an overall summary of each method, noting their required hazard information and other additional models/inputs, their perceived implementation complexity in addition to the relative accuracy observed for the results presented here, provided the initial IM_1 is an efficient one. Inevitably, these methods require computational tools for implementation, and some of these tools are provided in the associated GitHub repository, although the challenge of characterising suitable hazard inputs would nevertheless remain to be addressed.

Another important aspect not explored in this study, and which should form the basis of future research, is the issue of site dependence. All fragility or vulnerability functions and conversions here were derived for a single site location. How

TABLE 1 | Comparison of IM conversion methods.

	Method 1	Method 2a	Method 2b	Method 2c	Method 3	Method 4	Method 5
Required hazard information	Complete PSHA output for IM_2	Complete PSHA output for IM_2	Partial PSHA output for IM_2	Partial PSHA output for IM_2	Uniform hazard spectrum	Hazard curves for IM_1 and IM_2	Hazard curves for IM_1 and IM_2
Additional models/inputs	GMMs and correlation models	GMMs and correlation models	GMMs and correlation models	GMMs and correlation models	Dispersion value for IM_2	Dispersion value for IM_2	Dispersion value for IM_2
Implementation complexity	High	High	Moderate	Moderate	Low	Low	Low
Accuracy	High	High	High	High	Moderate	Moderate	Low

they extend to other regions with different tectonic environments remains to be confirmed, particularly given the influence of seismic hazard information in the conversion equations. In reality, site dependence also affects current fragility or vulnerability models, although it is seldom discussed. The degree to which these models are independent or sufficient with respect to site hazard depends largely on the chosen IM. Kohrangi et al. (2017) demonstrated site dependence for IMs such as $Sa(T)$, but also indicated that next-generation candidates like $Sa_{avg}(T)$ may exhibit site independence, offering substantial flexibility. If this finding is confirmed for the present study, the implications would be significant. The first implication is that analysts would be encouraged to adopt more efficient IMs, which would improve the accuracy of loss estimates. The second implication is that analysts would have greater flexibility when converting between models depending on the application, since earlier results have shown that more efficient IMs convert more reliably.

8 | Summary and Conclusions

This study examined how seismic fragility and vulnerability functions can be converted between different IMs. It reviewed various approaches available in the literature, ranging from assumptions based on uniform hazard equivalence, to the use of proxy structures, to applications of the total probability theorem. In addition, an alternative method based on the principle of uniform risk equivalence was trialled, along with refinements to the probabilistic approach to incorporate more detailed hazard information and nonspectral IMs such as filtered incremental velocity, $FIV3(T)$, and average spectral acceleration, $Sa_{avg}(T)$. These methods were comparatively discussed and collectively applied to many case study conversion scenarios for evaluation. The results of each possible conversion type were compared against a reference function to assess the efficiency of the conversion methods. This comparison was performed for fragility functions across several DSs, as well as for vulnerability functions describing the economic loss of the structure. Based on this analysis, the following conclusions can be drawn:

- Methods based on total probability tended to perform best across all conversions examined and should be employed when possible. Methods based on uniform hazard and uniform risk equivalence tended to be less accurate as they depended heavily on the relative efficiencies of the original IM and target IM. If they were equally efficient, simpler conversions requiring little hazard information worked reasonably well. If the original IM was inefficient, the conversion typically broke down, and not much could be done to convert it to an efficient IM. This was true for traditional IMs like PGA or $Sa(T)$, but next-generation IMs like $Sa_{avg}(T)$ and FIV3 showed good robustness when converting between themselves;
- When using period-dependent IMs, like $Sa(T)$ or $Sa_{avg}(T)$, fragility conversion from a higher period to a lower period tends to work well, but not the other way around, as previously noted by Suzuki and Iervolino (2020);
- The previous point implies that converting all spectral-based IMs to PGA is a reasonable solution and serves as a common convergence point for comparative analysis. This was observed to be the case, where accurate conversions to PGA could be made, but this still results in an inefficient IM that, when extended to vulnerability, results in overestimations of economic losses and therefore, is not advised;
- A very promising observation was made regarding the use of the next-generation IM $FIV3(T)$, since it has been shown by Aristeidou et al. (2025) to be highly correlated with itself and relatively independent of period, meaning a

single definition could be widely applied. The real benefit came from its high efficiency in characterising damage and its sufficiency with respect to site hazard. As the previous point suggests that PGA could be a common convergence point, making it a *universal receiver* to use blood transfusion terminology, FIV3(T) can be thought of as a *universal donor*, since fragility functions developed using this IM can be easily converted to other IMs without any significant implications on accuracy or bias. This restates the case for developing fragility/vulnerability models using such flexible IMs.

Lastly, although this work has focused on converting fragility/vulnerability functions to a common IM to enable collective analysis using a single GMF, recent work by Monteiro et al. (2026) has introduced several cross-IM spatial correlation models. These models can eliminate the need for such conversions, albeit with a modest increase in computational cost.

Acknowledgments

The ground motion record selections and hazard consistency verifications described here were performed using an academic licence of the Djura online ground motion record selector (www.djura.it). The work presented here has been developed within the framework of the "Sensor-driven statistical tools to evaluate risks and manage safety in the built environment" (SONATA) project, which is a Starting Grant awarded by the Italian Science Fund (Fondo Italiano per la Scienza) at IUSS Pavia under grant number FIS2023-03215. The comments and suggestions of Tomas Mejia, Vitor Monteiro in addition to three anonymous reviewers are also gratefully acknowledged.

Funding

This study was supported by Ministero dell' Università e della Ricerca (Grant FIS2023-03215).

Conflicts of Interest

The authors declare no conflicts of interest.

Data Availability Statement

Further information including extensive plots of all scenarios in addition to some computational tools are available at: https://github.com/djura-risk-data-engineering/fragility-vulnerability-im-conversion.

Endnotes

[1] Michel et al. (2018) mistakenly wrote the conditional distribution term in Equation (6) as $f_{\mathrm{IM}_2\,|\,\mathrm{IM}_1}$ instead of $f_{\mathrm{IM}_1\,|\,\mathrm{IM}_2}$.

References

Abarca, A., R. Monteiro, and G. J. O'Reilly. 2022. "Simplified Methodology for Indirect Loss-Based Prioritization in Roadway Bridge Network Risk Assessment." *International Journal of Disaster Risk Reduction* 74: 102948. https://doi.org/10.1016/j.ijdrr.2022.102948. https://linkinghub.elsevier.com/retrieve/pii/S2212420922001674.

Abarca, A., R. Monteiro, and G. J. O'Reilly. 2025. "Seismic Risk Prioritisation Schemes for Reinforced Concrete Bridge Portfolios." *Structure and Infrastructure Engineering* 21: 49–69. https://doi.org/10.1080/15732479.2023.2187424.

Ancheta, T. D., R. B. Darragh, J. P. Stewart, et al. "Nga-west2 Database." *Earthquake Spectra* 30, no. 3: 2014. 989–1005. https://doi.org/10.1193/070913eqs197m.

Aristeidou, S., and G. J. O'Reilly. 2024. "Exploring the use of Orientation-Independent Inelastic Spectral Displacements in the Seismic Assessment of Bridges." *Journal of Earthquake Engineering* 28: 3515–3538. https://doi.org/10.1080/13632469.2024.2343067.

Aristeidou, S., D. Shahnazaryan, and G. J. O'Reilly. 2024. "Artificial Neural Network-Based Ground Motion Model for Next-Generation Seismic Intensity Measures." *Soil Dynamics and Earthquake Engineering* 184: 108851. https://doi.org/10.1016/j.soildyn.2024.108851.

Aristeidou, S., D. Shahnazaryan, and G. J. O'Reilly. 2025. "Correlation Models for Next-Generation Amplitude and Cumulative Intensity Measures Using Artificial Neural Networks." *Earthquake Spectra* 41, no. 1: 851–875. https://doi.org/10.1177/87552930241270563.

Baker, J. W., and B. A. Bradley. 2017. "Intensity Measure Correlations Observed in the Nga-west2 Database, and Dependence of Correlations on Rupture and Site Parameters." *Earthquake Spectra* 33: 145–156. https://doi.org/10.1193/060716eqs095m.

Bradley, B. A. 2010. "A Generalized Conditional Intensity Measure Approach and Holistic Ground-Motion Selection." *Earthquake Engineering & Structural Dynamics* 39, no. 2: 1321–1342. https://doi.org/10.1002/eqe.995.

Bradley, B. A. 2012. "The Seismic Demand Hazard and Importance of the Conditioning Intensity Measure." *Earthquake Engineering & Structural Dynamics* 41: 1417–1437. http://doi.wiley.com/10.1002/eqe.2221.

Cornell, C. A., F. Jalayer, R. O. Hamburger, and D. A. Foutch. 2002. "Probabilistic Basis for 2000 Sac Federal Emergency Management Agency Steel Moment Frame Guidelines." *Journal of Structural Engineering* 128: 526–533. https://doi.org.10.1061/(ASCE)0733-9445(2002)128.

Crowley, H., J. Dabbeek, V. Despotaki, et al. 2021. "European Seismic Risk Model (esrm20)." *EFEHR Technical Report*, 002. https://doi.org/10.7414/EUC-EFEHR-TR002-ESRM20.

Dávalos, H., and E. Miranda. 2019. "Filtered Incremental Velocity: A Novel Approach in Intensity Measures for Seismic Collapse Estimation." *Earthquake Engineering & Structural Dynamics* 48: 1384–1405. https://doi.org/10.1002/eqe.3205.

Dávalos, H., and E. Miranda. 2020. "Evaluation of fiv3 as an Intensity Measure for Collapse Estimation of Moment-Resisting Frame Buildings." *Journal of Structural Engineering* 146: 04020204. https://doi.org/10.1061/(ASCE)ST.1943-541X.0002781.

Dávalos, H., and E. Miranda. 2021. "Robustness Evaluation of fiv3 Using Near-Fault Pulse-Like Ground Motions." *Engineering Structures* 230: 111694. https://doi.org/10.1016/j.engstruct.2020.111694.

Eads, L., E. Miranda, and D. G. Lignos. 2015. "Average Spectral Acceleration as an Intensity Measure for Collapse Risk Assessment." *Earthquake Engineering & Structural Dynamics* 44, no. 12: 2057–2073. https://doi.org/10.1002/eqe.2575.

Esposito, S., I. Iervolino, A. d'Onofrio, A. Santo, F. Cavalieri, and P. Franchin. 2015. "Simulation-Based Seismic Risk Assessment of Gas Distribution Network." *Computer-Aided Civil and Infrastructure Engineering* 30: 508–523. https://doi.org/10.1111/mice.12105.

Fox, M. J., P. J. Stafford, and T. J. Sullivan. 2016. "Seismic Hazard Disaggregation in Performance-Based Earthquake Engineering: Occurrence or Exceedance?." *Earthquake Engineering & Structural Dynamics* 45, no. 5: 835–842. https://doi.org/10.1002/eqe.2675.

Franchin, P., and F. Cavalieri. 2015. "Probabilistic Assessment of Civil Infrastructure Resilience to Earthquakes." *Computer-Aided Civil and Infrastructure Engineering* 30: 583–600. https://doi.org/10.1111/mice.12092.

Ghimire, S., P. Guéguen, and A. Astorga. 2021. "Analysis of the Efficiency of Intensity Measures from Real Earthquake Data Recorded in Buildings." *Soil Dynamics and Earthquake Engineering* 147: 106751. https://doi.org/10.1016/j.soildyn.2021.106751.

Goda, K., and H. P. Hong. 2008. "Spatial Correlation of Peak Ground Motions and Response Spectra." *Bulletin of the Seismological Society of America* 98: 354–365. https://doi.org/10.1785/0120070078.

Hellinger, E. 1909. "Neue Begründung der Theorie Quadratischer Formen Von Unendlichvielen veränderlichen (in German)." *Journal für Die Reine Und Angewandte Mathematik* 1909: 210–271. https://doi.org/10.1515/crll.1909.136.210.

Heresi, P., and E. Miranda. 2022. "Structure-to-Structure Damage Correlation for Scenario-Based Regional Seismic Risk Assessment." *Structural Safety* 95: 102155. https://doi.org/10.1016/j.strusafe.2021.102155. https://linkinghub.elsevier.com/retrieve/pii/S0167473021000783.

IBC. 2006. "International Building Code, Technical report." International Code Council.

Karaferis, N. D., and D. Vamvatsikos. 2022. "Intensity measure transformation of fragility curves for 2d buildings using simplified models." in Proceedings of the 3rd European Conference on Earthquake Engineering & Seismology (3ECEES). https://doi.org.10.5281/zenodo.15342810. https://lambdalab.ntua.gr/docs/conferences/Karaferis_Vamvatsikos_3ECEES.pdf.

Kazantzi, A. K., and D. Vamvatsikos. 2015. "Intensity Measure Selection for Vulnerability Studies of Building Classes." *Earthquake Engineering & Structural Dynamics* 44, no. 15: 2677–2694. http://doi.wiley.com/10.1002/eqe.2603.

Kohrangi, M., D. Vamvatsikos, and P. Bazzurro. 2017. "Site Dependence and Record Selection Schemes for Building Fragility and Regional Loss Assessment." *Earthquake Engineering & Structural Dynamics* 46: 1625–1643. https://doi.wiley.com/10.1002/eqe.2873.

Lin, T., C. B. Haselton, and J. W. Baker. 2013. "Conditional Spectrum-Based Ground Motion Selection. Part I: Hazard Consistency for Risk-Based Assessments." *Earthquake Engineering & Structural Dynamics* 42, no. 12: 1847–1856. http://doi.wiley.com/10.1002/eqe.2301.ISSN 00988847.

Luco, N., and C. A. Cornell. 2007. "Structure-Specific Scalar Intensity Measures for Near-Source and Ordinary Earthquake Ground Motions." *Earthquake Spectra* 23, no. 2: 357–392. https://doi.org/10.1193/1.2723158.

Martins, L., and V. Silva. 2021. "Development of a Fragility and Vulnerability Model for Global Seismic Risk Analyses." *Bulletin of Earthquake Engineering* 19, no. 15: 6719–6745. https://doi.org/10.1007/s10518-020-00885-1.

Mehdizadeh, M., K. R. Mackie, and B. G. Nielson. 2017. "Scaling Bias and Record Selection for Quantifying Seismic Structural Demand." *Journal of Structural Engineering* 143, no. 9: 04017117. https://doi.org/10.1061/(ASCE)ST.1943-541X.0001855.

Mejia, T., and G. J. O'Reilly. 2026. "Quantifying the Impacts of Incorporating Damage Correlation on Scenario-Based Regional Seismic Assessment." *Earthquake Engineering & Structural Dynamics* 55, no. 1: 94–111. https://doi.org/10.1002/eqe.70069.

Meletti, C., F. Galadini, G. Valensise, et al. 2008. "A Seismic Source Zone Model for the Seismic Hazard Assessment of the Italian Territory." *Tectonophysics* 450, no. 1: 85–108. https://doi.org/10.1016/j.tecto.2008.01.003.

Michel, C., H. Crowley, P. Hannewald, P. Lestuzzi, and D. Fah. 2018. "Deriving Fragility Functions from Bilinearized Capacity Curves for Earthquake Scenario Modelling Using the Conditional Spectrum." *Bulletin of Earthquake Engineering* 16, no. 10: 4639–4660. https://doi.org/10.1007/s10518-018-0371-3.

Monteiro, V. A., and G. J. O'Reilly. 2026. "A Review of Ground Motion Correlation Modelling for Regional Seismic Risk Analysis." *Bulletin of Earthquake Engineering* 24: 2497–2546. https://doi.org/10.1007/s10518-026-02377-0.

Monteiro, V. A., S. Aristeidou, and G. J. O'Reilly. 2026. "Spatial Cross-Correlation Models for Next-Generation Amplitude and Cumulative Intensity Measures." *Earthquake Spectra* 42, no. 2: https://doi.org/10.1002/esp4.70076.

Montemayor, D., E. Miranda, and H. Dávalos. 2025. "Evaluation of the Effects of Ground Motion Duration on Structural Collapse." *Earthquake Engineering and Structural Dynamics* 54: 2727–2747. https://doi.org/10.1002/eqe.4385.ISSN 10969845.

Montemayor, D., E. Miranda, and H. Dávalos. 2026. "Evaluation of the Adjustment of the Collapse Capacity by Epsilon in the Fema p-695 Methodology." *Earthquake Engineering & Structural Dynamics* 55, no. 9: 1865–1886. https://doi.org/10.1002/eqe.70169.

O'Reilly, G. J. 2021. "Seismic Intensity Measures for Risk Assessment of Bridges." *Bulletin of Earthquake Engineering* 19, no. 9: 3671–3699. https://doi.org/10.1007/s10518-021-01114-z.

O'Reilly, G. J., and D. Shahnazaryan. 2024. "On the Utility of Story Loss Functions for Regional Seismic Vulnerability Modeling and Risk Assessment." *Earthquake Spectra* 40, no. 3: 1933–1955. https://doi.org/10.1177/87552930241245940.

O'Reilly, G. J., and G. M. Calvi. 2020. "Quantifying Seismic Risk in Structures via Simplified Demand-Intensity Models." *Bulletin of Earthquake Engineering* 18: 2003–2022. https://doi.org/10.1007/s10518-019-00776-0.

Pagani, M., D. Monelli, G. Weatherill, et al. 2014. "Openquake Engine: An Open Hazard (and Risk) Software for the Global Earthquake Model." *Seismological Research Letters* 85, no. 3: 692–702. https://doi.org/10.1785/0220130087.

Pitilakis, K., P. Franchin, B. Khazai, and H. Wenzel. 2014. SYNER-G: Systemic Seismic Vulnerability and Risk Assessment of Complex Urban, Utility, Lifeline Systems and Critical Facilities. Vol. 31. Springer Netherlands. https://doi.org/10.1007/978-94-017-8835-9.

Rosti, A., C. D. Gaudio, M. Rota, et al. 2021. "Empirical Fragility Curves for Italian Residential Rc Buildings." *Bulletin of Earthquake Engineering* 19: 3165–3183. https://doi.org/10.1007/s10518-020-00971-4.

Shahnazaryan, D., and G. J. O'Reilly. 2024. "Next-Generation Non-Linear and Collapse Prediction Models for Short- to Long-Period Systems via Machine Learning Methods." *Engineering Structures* 306: 117801. https://doi.org/10.1016/j.engstruct.2024.117801. https://linkinghub.elsevier.com/retrieve/pii/S0141029624003638.

Shahnazaryan, D., V. Ozsarac, and G. J. O'Reilly. 2025. Djura ground motion record selector: A software solution for earthquake engineering." in COMPDYN. 2025- 10th ECCOMAS Thematic Conference on Computational Methods in Structural Dynamics and Earthquake Engineering.

Shome, N, C. Allin Cornell, P. Bazzurro, and Carballo J. E. 1998. "Earthquakes, Records, and Nonlinear Responses." *Earthquake Spectra* 14, no. 3: 469–500. https://doi.org/10.1193/1.1586011.

Silva, V., H. Crowley, and M. Colombi. 2014. *Fragility Function Manager Tool*. 385–402. Springer Netherlands. https://doi.org/10.1007/978-94-007-7872-6_13.

Stucchi, M., C. Meletti, V. Montaldo, H. Crowley, G. M. Calvi, and E. Boschi. 2011. "Seismic Hazard Assessment (2003–2009) for the Italian Building Code." *Bulletin of the Seismological Society of America* 101, no. 4: 1885–1911. https://doi.org/10.1785/0120100130.

Stucchi, M., P. Albini, M. Mirto, and A. Rebez. 2009. "Assessing the Completeness of Italian Historical Earthquake Data." *Annals of Geophysics* 47, no. 2-3: 1593–5213. https://doi.org/10.4401/ag-3330.

Suzuki, A., and I. Iervolino. 2020. "Intensity Measure Conversion of Fragility Curves." *Earthquake Engineering & Structural Dynamics* 49, no. 6: 607–629. https://doi.org/10.1002/eqe.3256.

Vamvatsikos, D. 2013. "Derivation of New Sac/Fema Performance Evaluation Solutions with Second-Order Hazard Approximation. "*Earthquake Engineering & Structural Dynamics* 42: 1171–1188. https://doi.org/10.1002/eqe.2265.

Weatherill, G. A., V. Silva, H. Crowley, and P. Bazzurro. 2015. "Exploring the Impact of Spatial Correlations and Uncertainties for Portfolio Analysis in Probabilistic Seismic Loss Estimation." *Bulletin of Earthquake Engineering* 13: 957–981. https://doi.org/10.1007/s10518-015-9730-5.